Innovative Concepts in Microwave Photonics

José Capmany, Salvador Sales, Ivana Gasulla, José Mora, Juan Lloret and Juan Sancho

Instituto de Telecomunicaciones y Aplicaciones Multimedia,
Universitat Politècnica de València,
8G Building - access D - Camino de Vera s/n - 46022 Valencia (Spain)
Corresponding autor: jcapmany@iteam.upv.es

Abstract

This paper reports the work carried by ITEAM researchers on novel concepts in the field of Microwave Photonics (MWP). It includes activities related to the general modelling of MWP systems, the use of novel multicore fibers and recent advances in the emergent and hot topic of integrated microwave photonics.

Keywords: Microwave Photonics, Multicore fibers, Integrated optics.

1. Introduction

Microwave photonics (MWP) [1-3], a discipline which brings together the worlds of radiofrequency engineering and optoelectronics, has attracted great interest from both the research community and the commercial sector over the past 30 years and is set to have a bright future [4]. The added value that this area of research brings stems from the fact that, on the one hand, it enables the realization of key functionalities in microwave systems that either are complex or even not directly possible in the radiofrequency domain and, on the another hand, that it creates new opportunities for information and communication (ICT) systems and networks.

While initially, the research activity in this field was focused towards defense applications, MWP has recently expanded to address a considerable number of civil applications, including cellular [5], wireless [6], and satellite [7] communications, cable television [8], distributed antenna systems [9], optical signal processing [10] and medical imaging [4]. Many of these novel application areas demand ever-increasing values for speed, bandwidth and dynamic range while at the same time require devices that are small, lightweight and low-power, exhibiting large tunability and strong immunity to electromagnetic interference. Despite the fact that digital electronics is widely used nowadays in these applications, the speed of digital signal processors (DSPs) is normally less than several gigahertz (a limit established primarily by the electronic sampling rate) so in order to preserve the flexibility brought by these devices and their limit constraints there is a need for equally flexible front-end analog solutions to precede the DSP. This situation is schematically depicted in figure 1, where the block that constitutes the analog signal processing engine is shown.

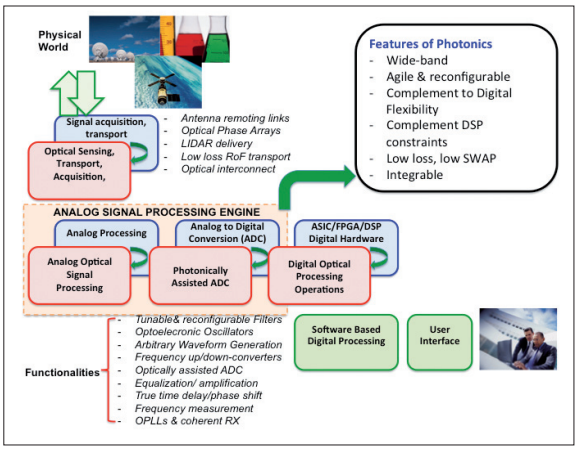

Figure 1. *The concept of analog signal processing engine in the context of information & communications systems.*

In this context, the unique capabilities offered by photonics makes MWP a promising alternative for wideband microwave signal processing bringing advantages in terms of Size, Weight And Power (SWAP) budgets.

One of the main driving forces for MWP in the middle term future is expected to come from broadband wireless access networks [4] installed in shopping malls, airports, hospitals, stadiums, power plants and other large buildings. The market for microwave photonic equipment is likely to grow with consumer demand for wireless gigabit services. For instance, the IEEE standard WiMAX (the Worldwide Interoperability for Microwave Access) has recently upgraded to handle data rates of 1 Gbit s^{-1}, and it is envisaged that many small, WiMAX-based stations or picocells will soon start to spring up. In fact, with the proliferation of tablet devices such as iPads, more wireless infrastructure will be required. Furthermore, it is also expected that the demand for microwave photonics will be driven by the growth of fibre links directly to the home and the proliferation of converged [11] and in-home networks [12]. To cope with this growth scenario, future networks will be expected to support wireless communications at data rates reaching multiple gigabits per second. In addition, the extremely low power consumption of an access network comprised of pico- or femtocells would make it much greener than current macrocell networks, which require high-power base stations.

Up to now, MWP signal processors and links have relied almost exclusively on discrete optoelectronic devices and standard optical fibres and fibre-based components which have been employed to support several functionalities listed in the lower left part of figure 1 [1-3, 10]. These configurations are bulky, expensive and power-consuming while lacking flexibility. Furthermore, the design of MWP systems is very much application-oriented and no general models have been developed which could be employed to develop general design rules, in particular for the evaluation of their performance metrics. In this context, ITEAM research activities in the field of MWP are being carried to address these important topics. On one hand, the issue of bulky MWP system configurations can be overcome by integration of MWP functionalities on a photonic chip and also, by reducing the interconnection complexity by means of using more efficient designs of optical fibers, which can provide the desired feature of parallelism and long range signal distribution with low losses. Integrated microwave photonics and the use of multicore optical fibers are cornerstones of these two novel paradigms respectively while analog filtered links recently proposed by ITEAM researchers providesd a unifying modelling approach of the different applications of MWP systems. In this paper we provide a descrition of these three innovative concepts.

2. Filtered analog links

2.1 Basic Principles

As mentioned in the introduction, Microwave Photonics (MWP) enables the transmission and processing of radiofrequency signals with unprecedent features as compared to other approaches based on traditional microwave technologies [1-3]. In telecommunications, MWP enables distributed antenna (DAS) and radio over fiber (RoF) systems, where broadband microwave and millimeter-waves are delivered from/to a central station to/from base stations with very low and frequency independent losses and limited distortion. In signal processing, MWP filters allow the processing and beamsteering of RF signals with features, like tunability and reconfigurability which are very difficult or even impossible to achieve with electronic circuits, while photonic analog to digital (ADC) converters bring the possibility of digitizing multi GHz broadband signals. Finally MWP systems allow as well the implementation of very versatile RF signal generators spanning from ultrawideband (UWB) to millimetre-wave signals through dedicated architectures and optoelectronic oscillators (OEOs). The performance of MWP systems has traditionally been assessed through a set of figures of merit (FOM), which include end-to-end RF gain, Noise Figure and Dynamic Range [13]. In most occasions, a specialised analysis is carried to assess a particular MWP application served by a particular architecture.

Very recently, several authors have proposed the concept of filtered MWP or analog links [14],[15] as a means to calculate the FOM values of more general MWP systems. This concept is shown in Figure 2 for a one input, one output port configuration, but can be readily extended to multiple input/output port architectures.

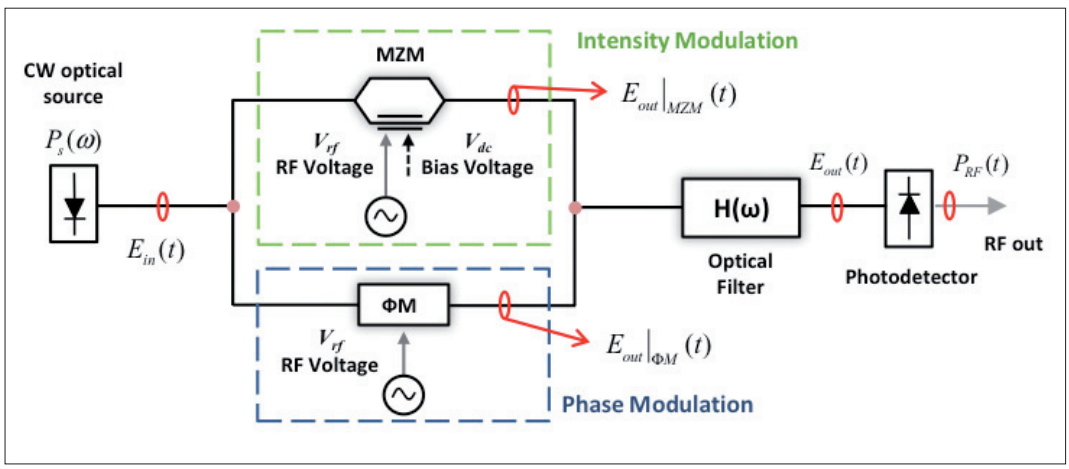

Figure 2. *Layout of a general single-port filtered MWP link.*

Here, either intensity or phase modulation (or both simultaneously) can be applied. The effect of all intermediate optical components placed between the electrooptical (EO) and the optical-to-electronic (OE) conversion stages can be lumped into an optical transfer function *H(ω)* connecting the input to the output of the system. The equations providing the values of the FOMs for this configuration have been derived in [14], including the possibility of using both monochromatic and modulated (non-zero linewidth) optical sources.

ITEAM researchers have demonstrated that filtered MWP links represent, in general any kind of MWP application/system and thus that the expressions derived in [14] can be employed to compute the FOMs in any kind of application context. Thus, filtered analog links constitute an unifying and generalistic model for MWP systems.

2.2 Examples of Filtered MWP systems

Perhaps the most direct analogy of a filtered MWP link and a particular application is that related to MWP filtering. For instance, Fig. 3 represents the typical scheme of a MWP filter.

An input RF signal (with spectrum sideband centered at frequency $\pm f_{RF}$ shown in point 1) coming from a generator or detected by means of a single or an array of antennas is used to modulate the output of an optical source which upconverts its spectrum to the optical region of the spectrum (point 2), such that the sidebands are now centered at $\pm f_{RF}$, where represents the central frequency of the optical source. The combined optical signal is then processed by an optical system composed of several photonic devices and characterized by an optical field transfer function $\mathrm{H}(\nu)$. The mission of the optical system is to modify the spectral characteristics of the sidebands so at its output they are modified according to a specified requirement as shown in point 3. Finally, an optical detector is employed to downconvert the processed sidebands again to the RF part of the spectrum by suitable beating with the optical carrier so the recovered RF signal, now processed (as shown in point 4) is ready to be sent to a RF receiver or to be re-radiated. The overall performance of the filter is characterized by an end-to-end electrical transfer function $\mathrm{H}(f_{RF})$, which links the input and output RF signals.

Microwave Photonics (MWP) enables the transmission and processing of radiofrequency signals with unprecedent features as compared to other approaches based on traditional microwave technologies.

Other MWP applications can also be cast under the model of filtered MWP links, such as the three systems displayed in Fig. 4. For instance, Fig. 4 (a) shows a RoF multipoint WDM network where each central station source/base station detector pair defines a different filtered MWP link characterized by the lumped optical transfer function that accounts for the effect of all the photonic components (including, naturally, the dispersive optical fiber). This configuration includes, as a special case, traditional single wavelength MWP links employed for other applications like distributed antenna systems (DAS), cellular communications etc. More specialized subsystems and applications are as well described by the filtered MWP link. For example, Fig. 4 (b) shows the particular case of an optoelectronic oscillator. Here the link is established between the electrical injection and electrical output ports. Initially, OEOs only included fiber delay lines as intermediate pho-

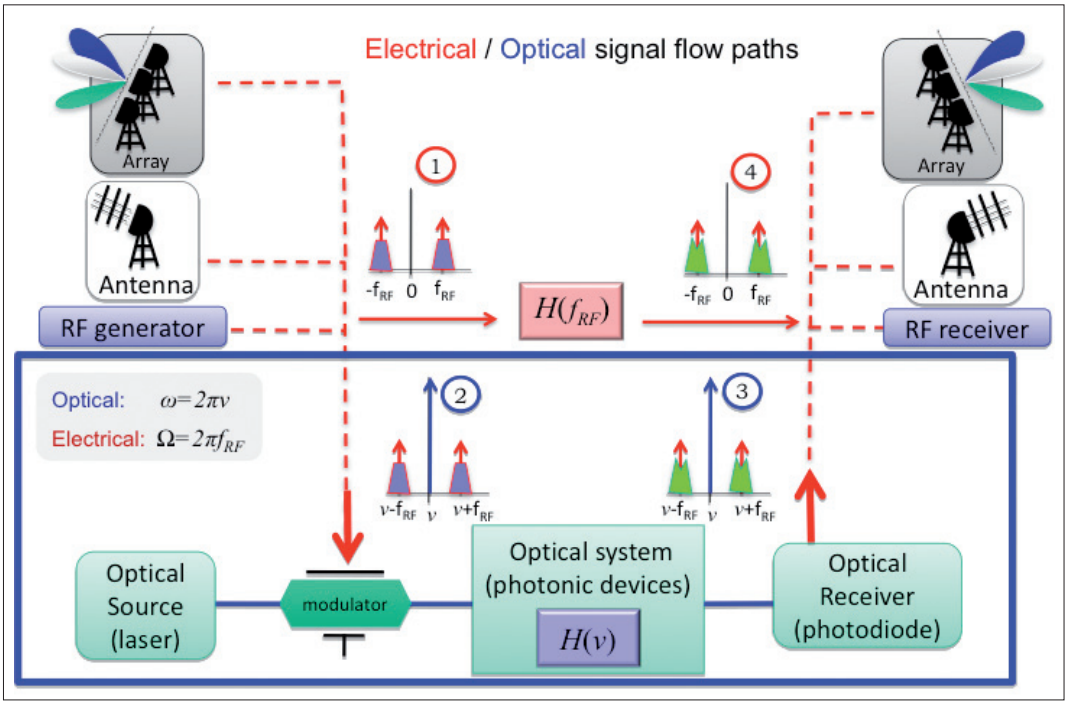

Figure 3. *Layout of a MWP Filter.*

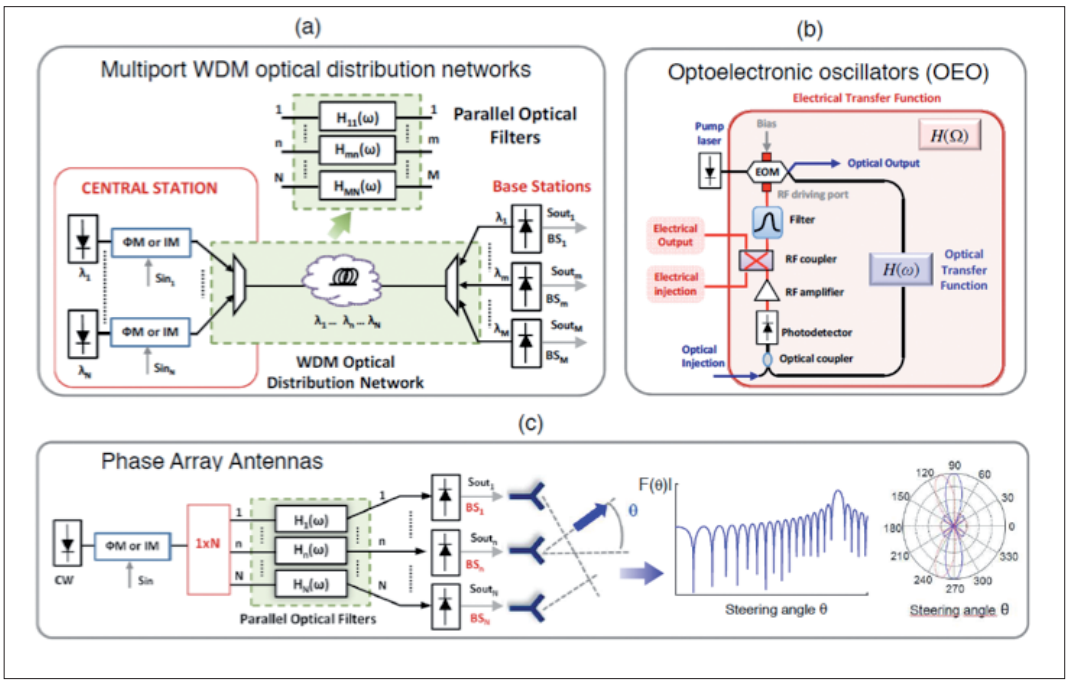

Figure 4. *Three examples of MWP applications and their equivalence to a filtered MWP link.*

tonic components. More recently other configurations including integrated and disk resonant cavities have also been proposed with a view of reducing the device footprint and thus open the possibility of potential integration on a chip. Figure 4 (c) shows the example of corresponding to optical beamsteering where spatial diversity defines an individual filtered MWP link channel between the source and each radiating element. In a similar way, the analogy can be established for other applications such as analog to digital conversion, frequency measurement, up and down-conversion, etc. For each particular application a different spectral configuration is required, but the underlying concept is the same.

2.3 Unified approach for MWP systems

The above examples suggest the possibility of unifying model for MWP systems based on the concept of filtered MWP link. Figure 5 shows the layout of the proposed configuration, which we call *general reconfigurable microwave photonic signal processor* (GMWPSP).

The proposed architecture embraces all the variety of applications in the field of MWP and each particular one is achieved by acting over the components in a different way as shown in Table 1. Performance values in terms of relevant parameters, such as bandwidth, losses, resolution and other figures of merit are very ap-

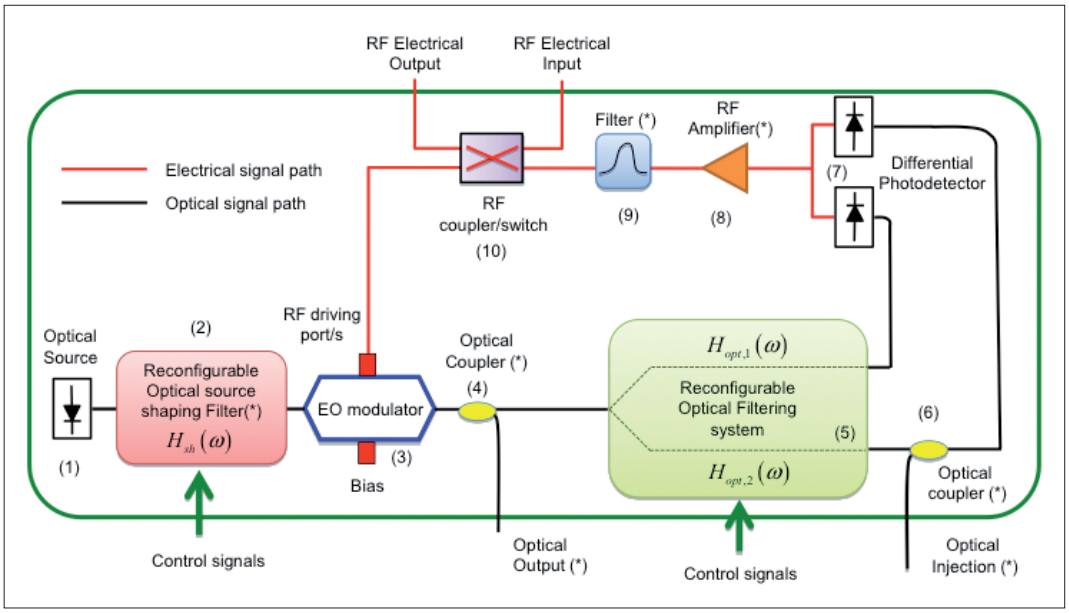

Figure 5. *General Reconfigurable Microwave Photonic Signal Processor.*

		Device in the MWPSP									
Functionality	**RF signal**	**(1)**	**(2)**	**(3)**	**(4)**	**(5)**	**(6)**	**(7)**	**(8)**	**(9)**	**(10)**
Filtering	Analog	L, TL, BS	FIR	IM, PM	-	FIR IIR DDL	-	S/D	(*)	(*)	X
AWG	Pulsed	L, BS		IM	-	FIR	-	S/D	(*)	-	X
ADC	Analog	BS	DDL	IM	-	DDL	-	S	(*)	-	X
OEO	Analog	L	-	IM, PM	(*)	IIR/ DDL	(*)	S	(*)	BPF	=
TBPS	Analog	L, TL	-	IM SSB	-	IIR	-	S	(*)	(*)	X
TTTD	Analog	L, TL	-	IM SSB	-	DDL	-	S	(*)	(*)	X
IFM	Analog	L	-	IM	-	FIR	-	D	(*)	(*)	X
FM	Analog	L	-	IM MBP	-	FIR	-	S	(*)	R	X
OPLL	Analog	L	-	IM/PM	R	-	R	S/D	-	R	X
FU/DC	Analog	L	-		R	FIR	R	D	-	R	X

Table 1. *Some of the MWP functionalities which can be implemented by the MWPSP. APPLICATION CODES. AWG: Arbitrary Waveform Generator, ADC: Analog to Digital Converter, OEO: Optoelectronic Oscillator, TBPS: Tunable Broadband Phase Shifter, TTTD: Tunable True Time Delay, IFM: Instantaneous Frequency Measurement. FM: Frequency Multiplication, OPLL: Optical Phase Locked Loop, FU/DC: Frequency Up/Down Converters. DEVICE CODES. L: Laser, TL: Tunable Laser, BS, Broadband Source, FIR: Finite Impulse Response, IIR: Infinite Impulse Response, DDL: Dispersive Delay Line, IM: Intensity Modulator, PM: Phase modulator, SSB: Single Sideband, MBP: Minimum Bias Point, S: Single Photodetector, D: Differential Photodetector, (*): Optional, BPF: RF Bandpass Filter, X: Electrical switch in Cross state, =: Electrical switch in Bar state, R: Required, -: Not Required.*

plication dependent. For instance, in the context of MWP signal filtering, typical values are RF gain around -10 dB, and Spurious Free Dynamic Range (SFDR) in the range of 90-100 dB. $Hz^{2/3}$, while in photonics ADC, this last figure is targeted at around 60-80 dB. $Hz^{2/3}$. In IFM a requency resolution of 1% of the central frequency is expected.

3. MWP applications of multicore fibers

3.1 Rationale

Multicore Fibers (MCFs), invented three decades ago [16], have been recently the subject of considerable attention and research [17-22] as they enable the increase in the transmission capacity of optical fiber links by spatial division multiplexing (SDM). Reported research has mainly addressed digital transmission systems in several contexts as long haul transmission [17], combined polarization, wavelength and spatial multiplexing domains [18-21] and passive optical networks (PONs) [22]. The inherent parallelism offered by MCFs with potential low or negligible signal coupling between their inner cores make them an ideal candidate for bandwidth extension in future telecommunication systems.

A vast majority of the research activity reported so far is based on the so-called homogeneous MCFs where identical cores are disposed in the fiber cross-section following different profiles in order to either suppress or have a given control over mode coupling. Fundamental design parameters are the core a and cladding b diameters, and

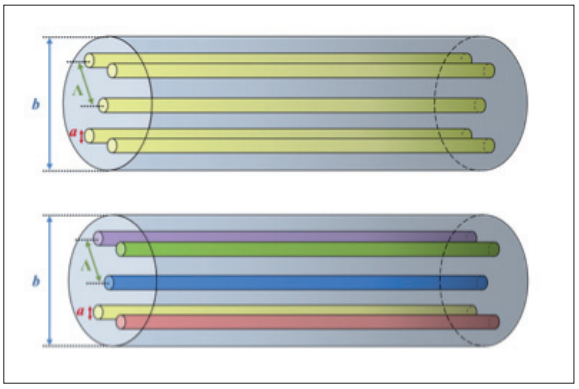

Figure 6. *Layouts for a homogeneous (upper) and heterogeneous (lower) multicore fiber including the relevant geometric design parameters.*

An unifying model for all MWP systems can be established based on the concept of filtered MWP link.

the core separation Λ, as shown in the upper part of figure 6. Designs including 7 cores have been proposed and reported in the literature [22] and there is also a considerable activity being displayed by several groups in order to understand which is the best geometry and material composition to optimize their performance [23,24].

There is an obvious interest in increasing the number of cores in MCFs, which requires the drastic reduction of mode coupling between the cores so they can be placed more tightly spaced within the cladding cross section. To this end, heterogeneous MCFs have been recently proposed [25]. In these, non-identical cores, which are singlemode in isolation of each other are arranged so, due to the absence of phase matching conditions, the crosstalk between any pair of cores is very small and thus can be more closely spaced. Although preliminary results have only been presented [26], MCFs with 19 and more cores are feasible and a broad field of design alternatives is expected to be proposed, both in terms of geometric designs as well as of material compositions, which will require a thorough analysis using coupled-mode theory models for MCFs [27].

In this section we describe the proposal for the potential application of MCFs to the implementation of a sampled discrete true time delay line for radiofrequency (RF) signals, which is the basis of multiple functionalities in the field of Microwave Photonics [2], [3]. We concentrate in particular on heterogeneous MCFs, where cores can be designed to have different dispersion profiles. Basic.

3.2 Heterogeneous Multicore Fibers

The basic building block of the proposed sampled optical delay line is based on an heterogeneous multicore fiber. Throughout the paper we assume, in consequence, that each core acts as an independent singlemode waveguide transmitting a fundamental mode. In particular, the fundamental mode of core *j* will have a propagation constant β_j , which we can approximate using a Taylor series around a central frequency of an optical source ω_0:

$$\beta_j(\omega) \approx \beta_j(\omega_0) + \left.\frac{d\beta_j(\omega)}{d\omega}\right|_{\omega=\omega_0} (\omega-\omega_0) + \frac{1}{2}\left.\frac{d\beta_j^2(\omega)}{d\omega^2}\right|_{\omega=\omega_0} (\omega-\omega_0)^2$$

$$= \beta_j^0 + \beta_j^1(\omega-\omega_0) + \frac{1}{2}\beta_j^2(\omega-\omega_0)^2 \quad [1]$$

In a similar way, the group delay of core *j* at a given wavelength $\tau_j(\lambda)$ will be expressed as:

$$\tau_j(\lambda) = L\,\frac{\lambda^2}{2\pi c}\,\frac{d\beta_j(\lambda)}{d\lambda} = L\left[\left.\frac{1}{v_{g,j}}\right|_{\lambda=\lambda_0} + D_j(\lambda-\lambda_0)\right] \quad [2]$$

where L is the fiber length, c the speed of light in vacuum, $v_{g,j} = 1\,\beta_j^1$ represents the group velocity in core *j* and D_j is the first order chromatic dispersion parameter of core *j* defined as:

$$D_j = -\frac{2\pi c}{\lambda^2}\,d\beta_j^2 \quad [3]$$

Next section describes the optical delay line operation and configuration principles by considering two possible implementation options. In first place we describe an implementation based on a heterogeneous MCF fed by a single input optical signal modulated by a RF subcarrier, where the different cores feature a different behavior in terms of chromatic dispersion. We then extend the concept to the case where the input is a RF modulated optical multicarrier signal fed to all the cores in the fiber.

3.3 MCF based Sampled Delay line Configurations

Figure 7shows the basic configuration and illustrates the operation principle of the discrete optical delay line for RF signals based on the use of a single input optical carrier.

As shown in the upper part of figure 7 the sampled delay line is composed of a single continuous wave (CW) laser source externally modulated (in amplitude or phase) by an input RF signal. The modulated input signal is then evenly distributed among the N cores of the heterogeneous MCF by means of a singlecore to multicore fiber coupler (SMC).

Although the different cores in the MCF have the same length L, we shall assume that each one features a linear group delay characteristic as a function of the wavelength with a different slope (i.e. a different first order chromatic dispersion parameter D_j) as shown in the lower part of figure 7. Under this linear group delay dependence, the group delay provided by each core can be approximated by:

$$\tau_j(\lambda) = \tau_0 + jDL(\lambda-\lambda_0) \quad [4]$$

where *D* represents a common first order chromatic dispersion parameter and τ_0 is a basic group delay common to all the cores for a given anchor or reference wavelength λ_0 , $\tau_0 = L/v_g$.

The basic incremental delay at a specific wavelength λ_k between the output signals from two cores featuring adjacent group delay characteristics is then given by:

$$T_k = \tau_{j+1}(\lambda_k) - \tau_j(\lambda_k) = DL(\lambda_k-\lambda_0) \quad [5]$$

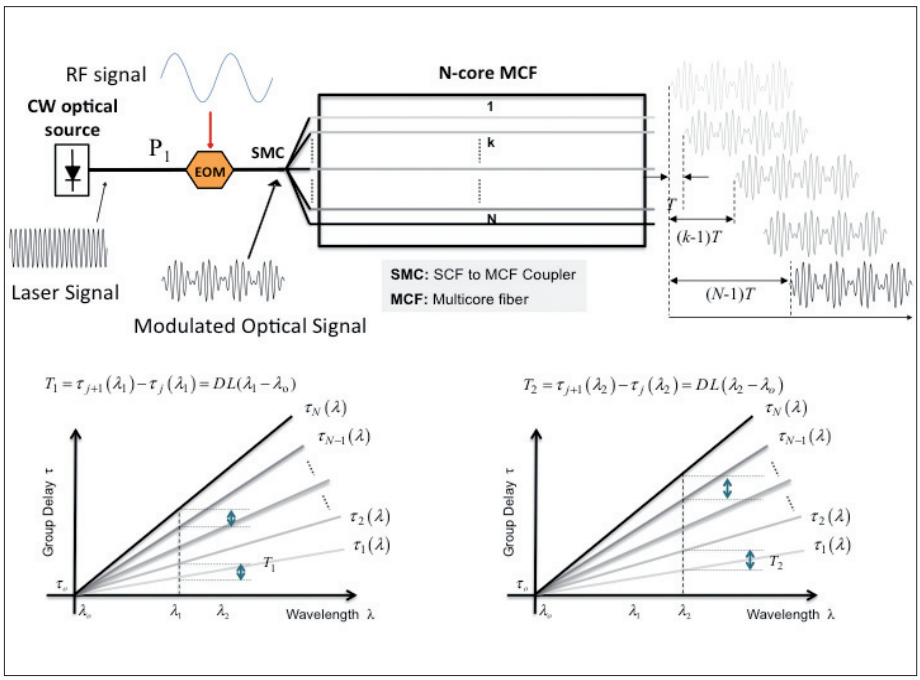

Figure 7. *Sampled delay line with spatial diversity output based on an heterogeneous MCF fed by a RF-modulated single optical carrier.*

This incremental group delay amount is fixed for a specific value of the wavelength. For example, the lower part of figure 7 shows the incremental group delay distribution when the operation wavelength is $_1$. In this case, the delay line produces N replicas of the input RF-modulated optical signal delayed respectively by 0, T_1, $2T_1$, … $(N-1)T_1$. To change the value of the basic incremental delay one needs to tune the wavelength of the input CW source. For example, the lower part of figure 7 illustrates the change in the value of the basic incremental delay $T_1 \rightarrow T_2$, when the input source wavelength is tuned from $\lambda_1 \rightarrow \lambda_2$. At the MCF output N equispaced samples (in time) of the input RF-modulated optical signal are thus obtained, featuring a tuneable basic intersample delay. Each sample is obtained at the output of a different core so we shall use the term of spatial diversity to identify this configuration.

An extension of the previous scheme where the input optical signal is of multicarrier nature (either by modelocking or by wavelength division multiplexing) is shown in figure 8. Referring to it the optical signal is composed by M carriers where the central wavelengths are given by $\lambda_i=\lambda_0+i\Delta\lambda$, $i=1,2\ldots M$. This multicarrier signal is then RF modulated and injected to all the cores of the heterogeneous MCF. In this way, as it can be observed in figure 9, each multiplex experiences, in each core j, a different basic incremental delay given by:

$$T_k=\tau_{j+1}(\lambda_k)-\tau_j(\lambda_k)=DL\Delta\lambda \qquad [6]$$

In other words, the output from each core corresponds to a sampled delay line providing M delayed samples where each core features a different basic incremental delay T_j.

This optical delay line actually provides a bidimesional delay configuration where the delay experienced by a RF signal sample carried by the wavelength $\lambda_i=\lambda_0+i\Delta\lambda$ and propagating through core j is given by:

$$T_{i,j}=\tau_0+ijDL\Delta\lambda \qquad [7]$$

This functionality can be exploited in two ways depending on whether the time or the wavelength domain is considered. In the first case, as it has been pointed before, the output of each core provides a different sampled delay line where the basic incremental delay is

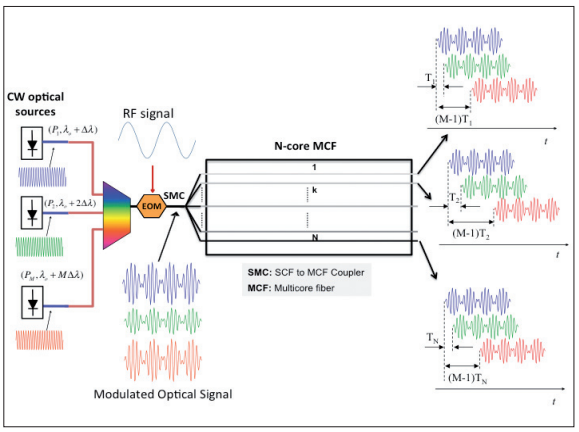

Figure 8. *Sampled delay line with spatial diversity output based on a heterogeneous MCF fed by a RF-modulated multiple optical carrier.*

obtained by fixing the value of j in (7) and then computing the difference between the delays experienced by wavelengths $i+1$ and i:

$$T_j = jDL\Delta\lambda \quad [8]$$

In this way spatial diversity enables the implementation of N independent delay lines, each one providing M samples and a different basic intersample delay.

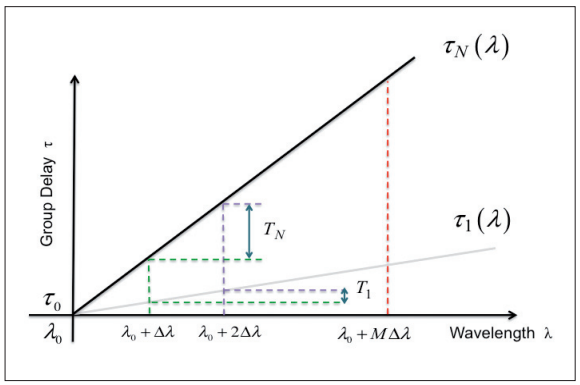

Figure 9. *Operation principle of the MWP optical delay line subject to multicarrier optical input RF-modulated signals. Illustration of the different incremental group delay obtained for each core.*

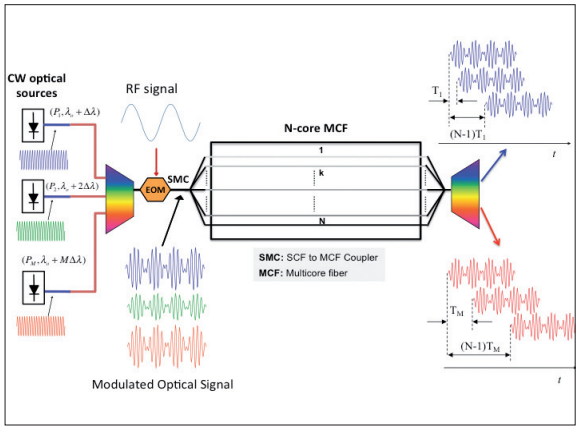

Figure 10. *Sampled delay line based on a heterogeneous MCF fed by a RF-modulated multiple optical carrier and WDM output demultiplexing.*

In the second case, which is illustrated in figure 10 the outputs from the *N* cores can be combined and wavelength demultiplexed to obtain *M* delay lines, each one featuring *N* samples, where the basic incremental delay in each line is given by:

$$T_j = jDL\Delta\lambda \quad [9]$$

3.4 Application to Arbitrary Waveform Generation

We consider the use of the MCF-based sampled delay lines to the generation of arbitrary waveforms. Although the discussion presented here can be generalized to other signal formats, we focuson the generation of ultrawideband (UWB) signals using the discrete time MWP signal processing approach reported in [10]. UWB signal generation is based on the generation, delay and combination of pulses with different polarity. This means that a MCF based system designed for this purpose must incorporate the possibility of producing positive and negative taps. Two different configurations based on a MCF fed by a single carrier can be envisaged.

The first one, shown in figure 11 employs two electrooptic modulators (EOM1 y EOM2) biased at their quadrature points but on opposite slopes $V_{dc,1}$ and $V_{dc,2}$, respectively. Both, are modulated by the same electrical input pulse. The modulated optical signalfrom EOM1 is injected to a set of N_1 cores of the MCF and will provide N_1 weighted and delayed positive replicas of the input pulse. On the other hand, the modulated optical waveform arising from EOM2 will be injected to a set of N_2 cores of the MCF providing N_2 weighted and delayed negative replicas of the input pulse. The final waveform synthesis is achieved by combining the outputs of the different cores in a single optical receiver. The flexibility of the generator in terms of sample delays follows the same roadmap as that required for tuning MWP filters, that is, by changing the value of the wavelength of the optical source the basic delay between pulse replicas can be modified.

In terms of sample polarity full flexibility can be achieved by incorporating $1xN$ couplers followed by 2x1 optical switches so, for a given sample, its polarity can be selected by activating the switch in cross or bar state. Fi-

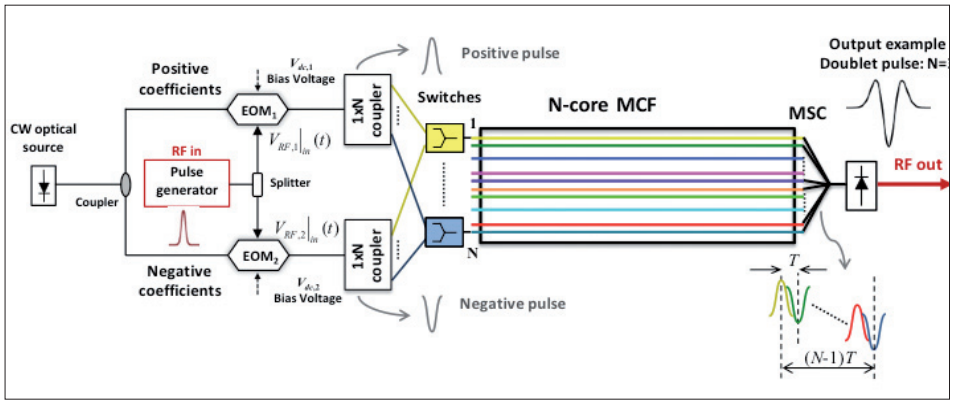

Figure 11. *Layout for the generation or arbitrary RF waveforms using a MCF and polarity inversion in Mach-Zehnder modulators.*

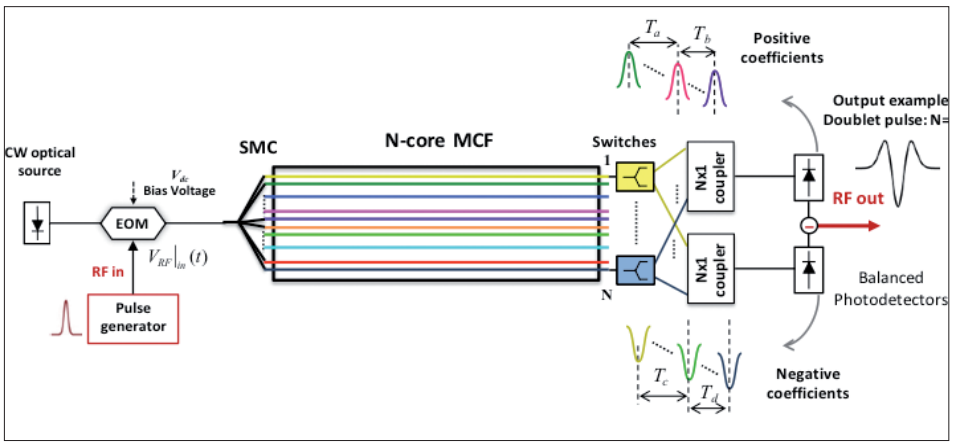

Figure 12. *Layout for the generation or arbitrary RF waveforms using a MCF and balanced differential detection.*

nally, it must be noted that the amplitude of each sample can be also controlled by placing attenuators at the outputs of the *1xN* couplers. As an example, figure 11 illustrates the case corresponding to the generation of a doublet pulse, $N=3(N_1=2, N_2=1)$, related to a sample amplitude weight vector [0.5,-1,0.5].

In the second approach, a single Mach-Zehnder modulator is employed and sample polarity is then implemented by means of a balanced differential detection preceded by 2x1 optical switching and *1xN* combination stages as shown in figure 12. The same principles described here for the generation of UWB pulses can be employed for other modulation formats such as pulse position modulation (PMM), bi-phase modulation (BPM), pulse amplitude modulation (PAM), ortogonal pulse modulation (OPM), etc.

4. Integrated MWP

4.1 State of the Art

Integrated Microwave Photonics (IMWP), which aims at the incorporation of MWP components/subsystems in photonic circuits, is an emergent area of research, considered as crucial for the implementation of both low-cost and advanced analog optical front-ends and, thus, instrumental to achieve the aforementioned evolution objectives.

IMWP is still in its infancy with sparse contributions being reported only recently which address either a very particular functionality or a limited set of devices. More specifically, efforts on the integration of MWP functionalities have been reported by several groups spanning III-V semiconductors [29],[30], hybrid [31] silicon [32],[33], and SiN (TripleX) [34] technologies. For example, in the context of filtering applications, most of the reported approaches are based on single cavity ring resonators. Results for a so-called unit cell, that could be an element of more complex lattice filters, have been reported in [35] for InP- InGaAsP. The same group has recently reported results of more complex designs as well as other different unit cell configurations [30]. A hybrid version incorporating silicon photonic waveguides has also been recently reported [31]. Another design based on cascading independently thermally controlled silicon rings has been presented demonstrating both second-order and fifth-order schemes [32]. A single SOI ring resonator has also been used in the implementation of multi-tap complex-valued filters [33], enabling tunability without changing the FSR. In SiN, a more elaborated design involving several rings and an interferometric structure has been proposed for exploiting in the development of both reconfigurable and tunable filtering tasks [34]. Other Microwave Photonic functionalities have also been demonstrated by partially using integrated circuits. For example, broadband tunable phase shifters and true time delay lines have been reported based on cascaded SOA devices [35], [36], passive silicon on insulator [37], and SiN [38] optical rings, and passive III-V photonic crystal waveguides [39]. Primary attempts for arbitrary waveform generators have been recently reported in CMOS compatible silicon [40]. We now describe the advances that have been obtained by ITEAM researchers in this particular area.

4.1 Microwave Photonic Signal Processor based on PhC waveguides

The suitability of exploiting the dispersive feature of a PhC-based delay has been demonstrated so as to per-

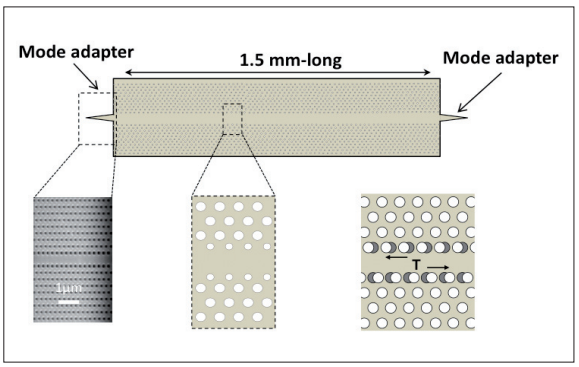

Figure 13. *PhC waveguide design including SEM image of the tapered coupler at the beginning of the waveguide, the smaller radius and the anti-symmetric shift of the first row of holes.*

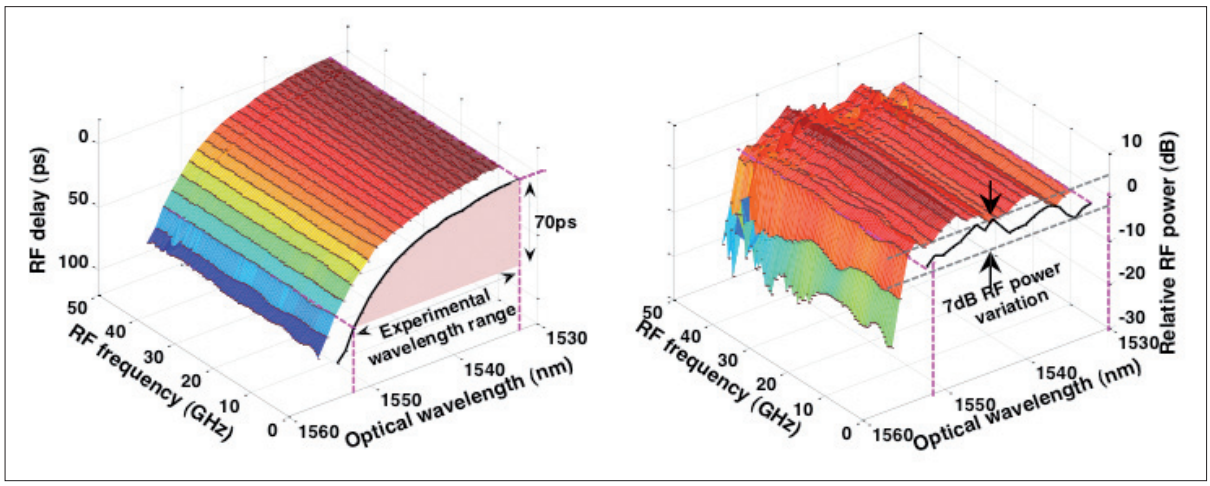

Figure 14. *Measured RF (a) phase shift and (b) power variation as a function of the RF frequency when the carrier wavelength is swept from 1532 to 1555 nm.*

form microwave photonic filtering tasks with unique performance in terms of bandwidth and delay-length ratio.

The waveguide design is shown in figure 13. The total length of the structure is 1.5 mm. The design consists of a triangular lattice of air holes with a period a of ~ 482 nm, and hole radius of ~ 0.26a. The first row of holes performances a slightly smaller radius (~ 0.25a), as it can be shown in the figure inset. The waveguide exhibits reduced loss in the slow light regime as a result of both design and fabrication optimization. The main idea was to apply an anti-symmetric shift of the first row of holes along the waveguide axis by ~ 0.15a, as illustrated in the figure inset. Besides, the fabricated device contains mode adapters [41], reducing, in such a way, the total insertion loss to about 8 dB (from fiber to fiber).

The performance of the PhC acting as a RF signal delay line was characterized by measuring both the RF power and phase shift in the RF domain when inserting the device into a MWP link [42]. The output wave of a tunable laser was used as the optical carrier of the MWP link. The RF signal was fed into the link through a Mach-Zehnder electro-optic modulator (MZM), which modulates the optical carrier intensity. Polarization controllers were deployed so as to adjust the polarization state at the input of the MZM and PhC waveguide. Lensed fibers were used for input and output optical coupling. A high-speed photodetector was followed by an RF amplifier in order to compensate for the loss introduced by the MWP link. The power and phase variations of the waveguide from 10 MHz to 50 GHz were characterized by means of a two-port vector network analyzer (VNA) whose output and input ports were respectively connected to the MZM RF input and the RF amplifier output.

Figure 14 depicts the measured delay and power variation of the PhC waveguide over the full RF frequency range for optical carrier wavelength ranging from 1532 to 1555 nm. As observed in figure 14(a), the group delay varies according to the tuning of the optical wavelength, resulting in 100 ps delay tunability for a 33 nm optical bandwidth. On the other hand, figure 14(b) shows a power variation of 7 dB, corresponding to a 3.5 dB change of the optical transmission, which was experienced by the RF signal while tuning the delay up to 70 ps. This delay was accomplished by sweeping the carrier wavelength from 1532 nm to 1552 nm. As it is clearly observed, further delays turn in a detrimental RF power response. This can be explained as follows: the impact of disorder results in a fast modulation of the optical transmission spectra, which in principle translates into a distorted transfer function of the microwave

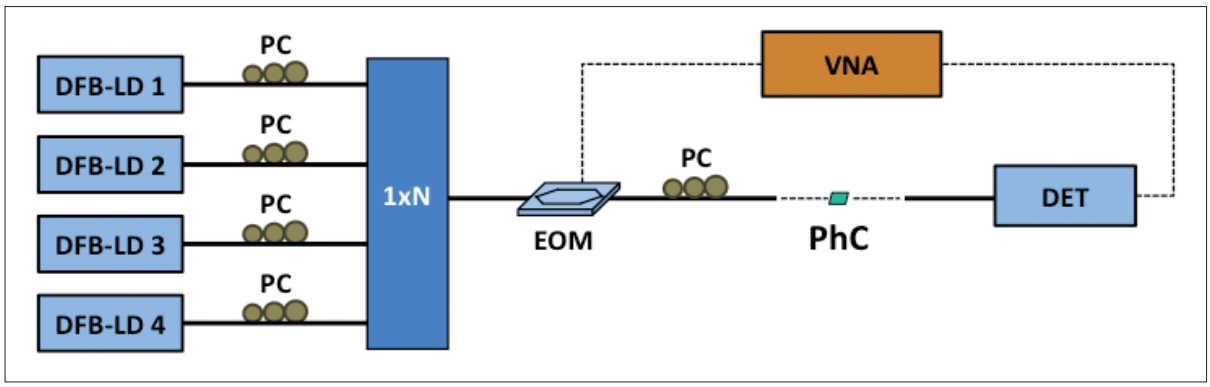

Figure 15. *Experimental layout of four-tap MWP filter comprising four optical sources and a PhC waveguide acting as a dispersive element.*

link. However, this effect is only noticeable when the delay is increased above 80 ps. It is important to mention that these measured results are referenced to a first acquisition performed at the lowest optical wavelength, corresponding to a fast propagation regime in the PhC waveguide.

The common implementation of a MWP FIR filter is that based on combining at the output a finite set of delayed and weighted replicas of the input optical intensity signal by means of a set of N non-dispersive optical fiber coils [10]. However, this scheme does not allow for an easy tuning, as it requires changing the value of the delay T in each tap of the filter. An alternative approach is that based on the combination of a dispersive delay line and different optical carriers where the value of the basic delay T is changed by tuning the wavelength separation among the carriers, thereby allowing tunability [43]. While in the first case the intensity or weight of each tap, represented by a_k, can be changed by inserting loss/gain devices in the different branches, with the second approach ak is readily adjusted by changing the optical power emitted by the optical sources [43]. This work has focusesed on this last approach since it becomes more flexible.

The generic layout of the four-tap PhC-based MWP filter assembled by combining four tunable lasers prior to modulation with the RF signal is illustrated in figure 15. Four replicas of the microwave signal, polarized along the slow axis (TE mode), will effectively propagate through the PhC with different delays, which are set to be equally time-spaced (with time shift T) by suitably setting the wavelengths of the four optical carriers. This principle is illustrated in figure 16. The uncorrelated nature of the four lasers guarantees the incoherent operation regime of the MWP filter. Thus, the electrical signal generated by the photodiode at the output of the PhC waveguide will result into the incoherent sum of the optical intensities of the four taps.

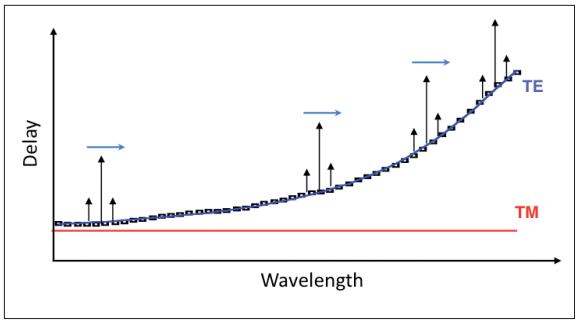

Figure 16. *Detail of the spectral placement for all the four taps within the TE delay profile.*

The corresponding transfer function of such a filter can be expressed as [10]:

$$H(f) = \sum_{k=0}^{3} a_k e^{-j k \left[\frac{2\pi f}{FSR}\right]} \qquad [9]$$

where $FSR = 1/T$. a_k can be adjusted by controlling the relative intensities of the tunable lasers. In the experimental demonstration reported here, all the filter taps a_k were set to the same power level (i.e. uniformly apodized filter), but coefficients variation, leading to transfer function reconfiguration is straightforward. Hence, with a single tunable delay line with a maximum delay τmax and N taps, the FSR can be tuned from $(N-1)/\tau_{max}$ to infinity. The experimental results are reported in figure 17, which are in very good agreement with numerical calculations. As the group delay is limited to 80 ps, the minimum FSR of the filter is 40 GHz. The FSR has been tuned from 40 to 70 GHz. The maximum extinction of the signal due to notch cancellation reaches 50 dB. Around 12 dB of main to secondary side-lobe (MSSL) ratio is obtained, which can be further enhanced by windowing the filter taps. In addition, very low distortion of the RF signal is observed over the broad spectral range (0 - 50 GHz).

Integrated Microwave Photonics (IMWP), which aims at the incorporation of MWP components/subsystems in photonic circuits, is crucial for the implementation of both low-cost and advanced analog optical front-ends.

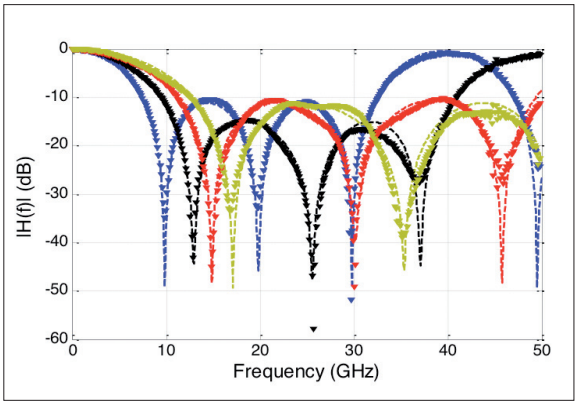

Figure 17. *Calculated (dashed lines) and measured (symbols) results for the filter response with different spectral scenarios of the emission wavelengths.*

4.2 Microwave Photonic Signal Processor based on III-V-on-Si microdisk resonator

To date, III-V/SOI microdisk resonators (MDR) have been used to develop several all-optical signal processing involving digital data signals [44]. However, the potential of III-V/SOI based MDR enabling MWP functionalities was unexplored so far. Recently, the suitability of exploiting this device in the implementation of photonic-assisted RF phase shifters and tunable filters have been demonstrated [45].

A schematic drawing of the III-V/SOI MDR structure is sketched in Fig. 18(a). It basically consists of an InP disk cavity, which is integrated on and coupled to a SOI nanophotonic waveguide. The cavity is bonded on the SOI circuit by using benzocyclobutene (BCB). Metal contacts are used for controlling the free carrier injection into de semiconductor cavity. The optical signal propagating through the Si waveguide is evanescently coupled into the disk cavity. The propagation inside the cavity relies on the so-called whispering gallery modes (WGM), which are confined on the edges of

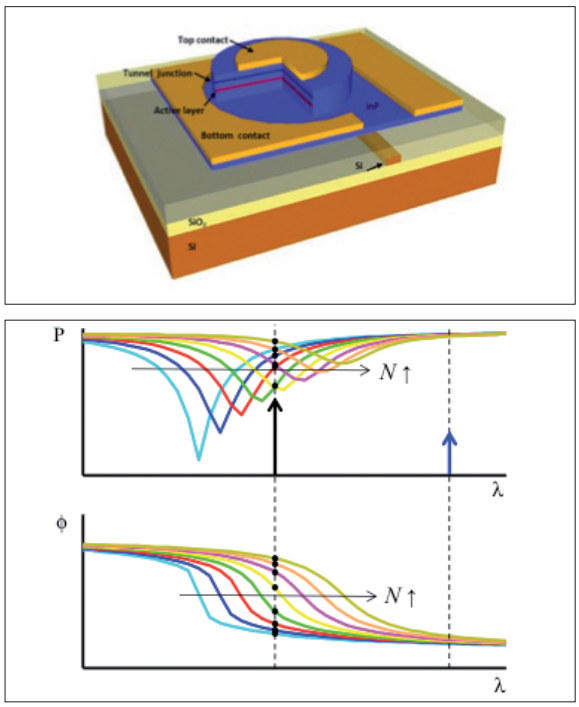

Figure 18. *(a) Schematic drawing of the III-V/SOI MDR structure. (b) Principle of operation as a photonic RF phase shifter.*

the disk resulting in a resonant-type transfer function. The principle of operation as a MWP phase shifter is based on using optical single sideband (OSSB) modulation in combination with an over-coupled MDR, which enables a 2π phase shift at each noth position. By acting on the carrier density in the InP cavity, the effective index can be modified. As a consequence, the spectral placement of the notches can be shifted. This way the phase induced on the optical carrier can be continuously adjusted, which at the end results in the phase control of the RF signal. This concept is shown in Fig. 18(b).

Figure 19(a) shows the spectral placement for both the optical carrier and the modulation sideband within the amplitude and phase transfer functions in the vicinity of a resonance. An effective index modification is translated into an spectral shift of the notch spectral position mediated by a change of the current injected into the MDR.

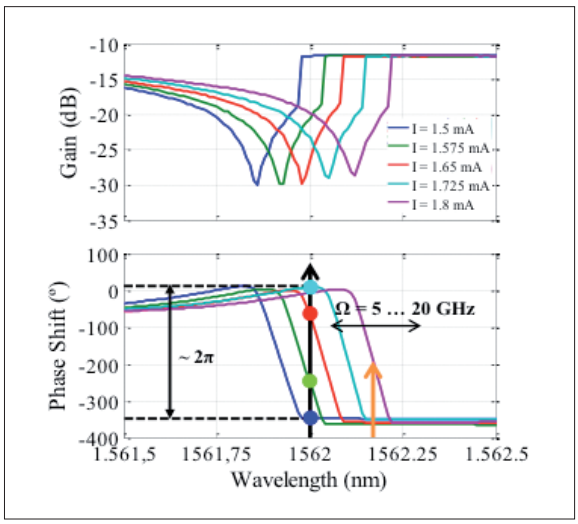

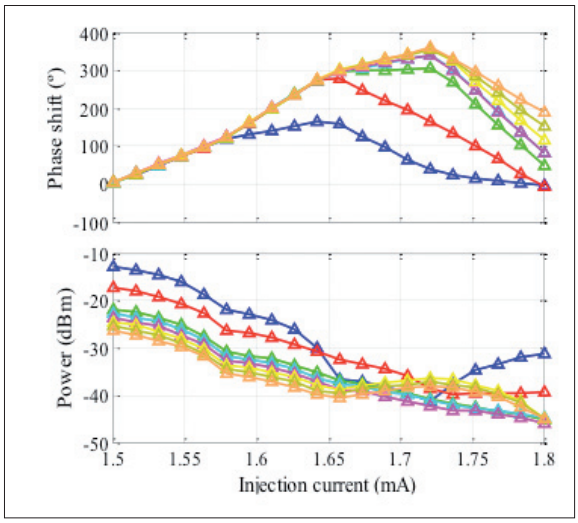

Figure 19. *(a) Amplitude and phase transfer functions of the MDR. (b) Phase shift and power variation of the output RF signal.*

The functionality as a MWP RF phase shifter in terms of phase shift and power variation for different RF frequencies is demonstrated and results are shown in Fig. 19(b). In this particular case, a minimum frequency of 18 GHz is required to reach quasi-linear and continuously tunable 360° phase-shifts. This minimum frequency is at the end

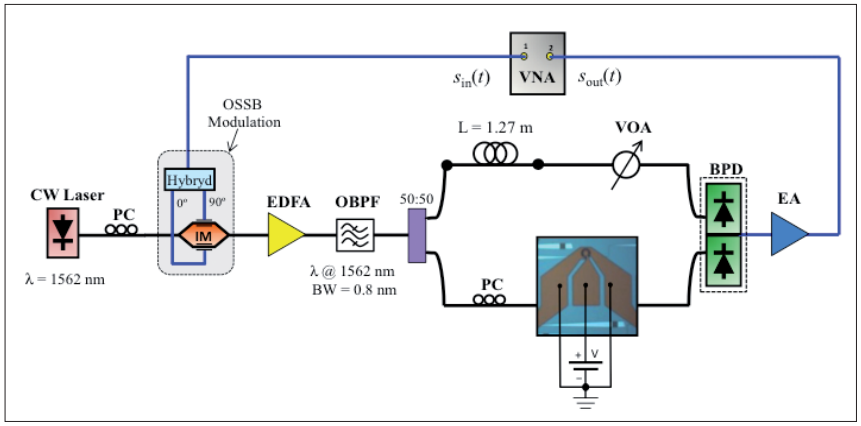

Figure 20. *Experimental setup of the complex-valued two-tap MWP tunable filter.*

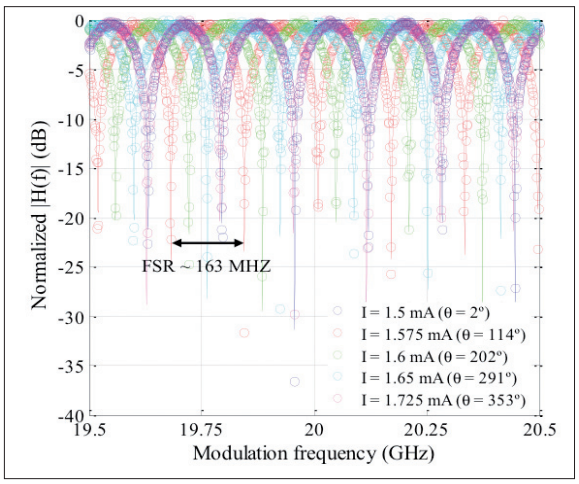

Figure 21. *Normalized frequency response of the MWP tunable filter for different injection currents.*

imposed by the phase slope abruptness, which is mainly governed by the power coupling status between the cavity and waveguide. In this approach, the tunability speed is limited by the carrier dynamics in the InP compound (hundreds of ps), which results in a great enhancement with respect to other SOI-based solutions [37]. Moreover, it is the most compact MWP fully tunable phase shifter reported up to now.

After demonstrating the suitability of III-V-on-Si MDRs for the purpose of developing RF phase shifting tasks, it has been used as a key element in the implementation of MWP transversal filters with complex-valued taps. Complex-valued taps in finite impulse response (FIR) schemes enables controllable basic phase shift, which results in response tunability without altering the FSR [10].

Figure 20 shows the experimental setup for the MDR-based MWP filter. The MDR is inserted in the lower arm of the interferometric structure. In this manner, the basic phase shift between both taps can be controlled by properly adjusting the injection current into the MDR. The interferometric structure is characterized by a length imbalance of 1.27 m, which corresponds to a notch-type response with a FSR of roughly 163 MHz. Both the calculated and measured filter responses are depicted in Fig. 21, showing good agreement. A center frequency of 20 GHz and an operating bandwidth of 1 GHz have been chosen, i.e. from 19.5 GHz to 20.5 GHz. Nearly 2π controllable basic phase shift (θ) over the operating bandwidth leads to continuously ~ 100% fractional tuning of the filter response with a rejection greater than 25 dB.

5. Summary and conclusions

We have reported the work carried by ITEAM researchers on novel concepts in the field of Microwave Photonics (MWP). The paper has described the progress in three main areas, including the general modelling of MWP systems by means of the so-called analog filtered links, the use of novel multicore fibers for the implementation of sampled RF optical delay lines and finally recent advances in the emergent and hot topic of integrated microwave photonics. The work on the two last topics is still in its preliminaries and it is expected that further and substantial progress will be reported in the coming months.

References

[1] A. Seeds, "Microwave photonics," IEEE Trans. Microwave Theory Tech. Vol. 50, pp. 877–887 (2002).
[2] J. Capmany and D. Novak, "Microwave photonics combines two worlds," Nature Photonics Vol. 1, pp. 319–330 (2007).
[3] J. Yao, "Microwave Photonics," J. Lightwave Technol. Vol. 27, pp. 314–335 (2009).
[4] See special Technology Focus on Microwave Photonics, Nature Photonics, Vol. 1, pp. 723-736 (2011).
[5] H. Al-Raweshidi and S. Komaki (Eds), Radio Over Fiber Technologies for Mobile Communications Networks, Artech House, Boston (2002).
[6] M. Mjeku and N. J. Gomes, "Performance analysis of 802.11e transmission bursting in fiber-fed networks," in Radio and Wireless Symp., pp. 133–136. (2008).
[7] M. Sotom, B. Benazet, A. Le Kernec, M. Maignan, 'Microwave Photonic Technologies for Flexible Satellite Telecom Payloads' in Proc. 35th European Conference on Optical Communication, 2009. ECOC '09. Pp. 1-4, Vienna (2009).
[8] W.I. Way, Broadband Hybrid Fiber/Coax Access System Technologies, Artech House, San Diego, (1998).
[9] M Crisp, R V Penty, I H White, A Bell, 'Wideband Radio over Fiber Distributed Antenna Systems for Energy Efficient In-Building Wireless Communications' In Proc. 2010 IEEE 71st Vehicular Technology Conference, Taipei, Taiwan, pp. 1-5 (2010).
[10] J. Capmany, B. Ortega, and D. Pastor, "A tutorial on microwave photonic filters," J. Lightw. Technol., Vol. 24, no. 1, pp. 201–229 (2006).
[11] M. Popov, "The convergence of wired and wireless services delivery in access and home networks", Invited, Conference on Optical Fiber Communication (OFC/NFOEC), (2010).
[12] A. M. Koonen, M. G. Larrode, A. Ng'oma, K. Wang, H. Yang, Y. Zheng, and E. Tangdiongga, "Perspectives of Radio-over-Fiber Technologies," in Optical Fiber Communication Conference, paper OThP3, (2008).
[13] C. H. Cox III, Analog Photonic Links: Theory and Practice, Cambridge University Press, Cambridge, U.K., 2004.
[14] I. Gasulla, J.Capmany: Analytical model and figures of merit for filtered microwave photonic links," Opt. Express, vol. 19, pp. 19758-19774, 2011.
[15] J. M. Wyrwas, Ming C. Wu: Dynamic Range of Frequency Modulated Direct-Detection Analog Fiber Optic Links, J. Lightwave Technol., vol. 27, pp. 5552-5562, 2009.
[16] S. Inao, T. Sato, S. Sentsui, T. Kuroha, and Y. Nishimura, "Multicore optical fiber," in Optical Fiber Communication 1979 OSA Technical Digest, paper WB1, 1979.
[17] T. Hayashi, T. Toshiki, S. Osamu, S. Takashi, and S. Eisuke, "Ultra-low-crosstalk multicore fiber feasible to

ultra-long haul transmission", in OFC/NFOEC 2011, paper PDPC, 2011.
[19] J. Sakaguchi, Y. Awaji, N. Wada, A. Kanno, T. Kawanishi, T. Hayashi, T. Taru, T. Kobayashi, and M. Watanabe, "109-Tb/s (7x97x172-Gb/s) SDM/WDM/PDM) QPSK transmission through 16.8-km homogeneous multicore fiber", in OFC/NFOEC 2011, paper PDPB6, 2011.
[20] B. Zhu, T.F. Taunay, M. Fishteyn, X. Liu, S. Chandrasekhar, M. F. Yan, J. M. Fini, E.M. Monberg, F.V. Dimarcello, K. Abedin, P.W. Wisk D.W. Peckham, and P. Dziedzic, "Space-, wavelength-, polarization-division multiplexed transmission of 56-Tb/s over a 76.8-km seven-core fiber", in OFC/NFOEC 2011, paper PDPB7, 2011.
[21] J. Sakaguchi et al., "Propagation characteristics of seven-core fiber for spatial and wavelength division multiplexed 10-Gbit/s Channels," in OFC/NFOEC 2011, paper OWJ2, 2011.
[22] B. Zhu, T.F. Taunay, M. Fishteyn, X. Liu, S. Chandrasekhar, M. F. Yan, J. M. Fini, E. M. Monberg, and F. V. Dimarcello,"112-Tb/s Space-division multiplexed DWDM transmission with 14-b/s/Hz aggregate spectral efficiency over a 76.8-km seven-core fiber," Opt. Express, vol. 19, no. 17, pp. 16665–16671, 2011.
[23] B. Zhu, T. F. Taunay, M. F. Yan, J. M. Fini, M. Fishteyn, E. M. Monberg, and F. V. Dimarcello, "Seven-core multicore fiber transmissions for passive optical network," Opt. Express, vol. 18, no. 11, pp. 11117–11122, 2010.
[24] K. Imamura, Y. Tsuchida, K. Mukasa, R. Sugizaki, K. Saitoh, and M. Koshiba, "Investigation on multi-core fibers with large Aeff and low micro bending loss," Opt. Express, vol. 19, pp. 10595-10603, 2011
[25] K. Takenaga, Y. Arakawa, S. Tanigawa, N. Guan, S. Matsuo, K. Saitoh, and M. Koshiba, "Reduction of crosstalk by trench-assisted multi-core fiber", in OFC/NFOEC 2010, paper OWk7, (010.
[26] M. Koshiba, K. Saitoh, and Y. Kokubun, "Heterogeneous multi-core fibers: proposal and design principle", IEICE Electron. Express, vol. 6, pp. 98-103, 2009.
[27] Y. Kokubun and T. Watanabe, "Dense heterogeneous uncoupled multi-core fiber using 9 types of cores with double cladding structure", 17th IEEE Microopics Conference (MOC), pp. 1-2, 2011.
[28] M. Koshiba, K. Saitoh, K. Takenaga, and S. Matsuo, "Multi-core fiber design and analysis: coupled-mode theory and coupled-power theory", Optics Express, vol. 19, pp. B102-B111, 2011.
[29] E.J. Norberg, R.S. Guzzon, S. Nicholes, J.S. Parker, and L. A. Coldren, "Programmable photonic filters fabricated with deeply etched waveguides," IPRM '09, paper TuB2.1, Newport Beach (2009).
[30] E. J. Norberg, R. S. Guzzon, J. Parker, L. A. Johansson, and L.A. Coldren, "Programmable photonic microwave filters monolithically integrated in InPInGaAsP," J. Lightw. Technol., Vol. 29, pp.1611–1619 (2011).
[31] H.W. Chen et al, "Integrated Microwave Photonic Filter on a Hybrid Silicon Platform", IEEE Transactions on Microwave Theory and Techniques, Vol 58, pp. 3213-3219 (2010).
[32] P. Dong, et al., "GHz-bandwidth optical filters based on high-order silicon ring resonators," Opt. Express Vol. 18, pp. 23784-23789 (2010).
[33] J. Lloret, J. Sancho, M. Pu, I. Gasulla, K. Yvind, S. Sales and J. Capmany, "Tunable complex-valued multi-tap microwave photonic filter based on single silicon-on-insulator microring resonator," Opt. Exp. Vol. 19, pp. 12402–12407 (2011).
[34] D. Marpaung, C. Roeloffzen, A. Leinse, and M. Hoekman, "A photonic chip based frequency discriminator for a high performance microwave photonic link," Opt. Express Vol. 18, pp. 27359-27370 (2010).
[35] W. Xue, S. Sales, J. Capmany, and J. Mørk, "Wideband 360° microwave photonic phase shifter based on slow light in semiconductor optical amplifiers," Opt. Express Vol. 18, pp. 6156-6163 (2010).
[36] P. Berger, J. Bourderionnet, F. Bretenaker, D. Dolfi, and M. Alouini, "Time delay generation at high frequency using SOA based slow and fast light," Opt. Express Vol. 19, pp. 21180-21188 (2011).
[37] M. Pu, L. Liu, W. Xue, Y. Ding, H. Ou, K. Yvind, and J. M. Hvam, "Widely tunable microwave phase shifter based on silicon-on-insulator dual-microring resonator," Opt. Express Vol. 18, pp. 6172-6182 (2010).
[38] M. Burla, D. Marpaung, L. Zhuang, C. Roeloffzen, M. R. Khan, A. Leinse, M. Hoekman and R. Heideman, "On-chip CMOS compatible reconfigurable optical delay line with separate carrier tuning for microwave photonic signal processing," Opt. Express Vol.19, pp. 21475–21484 (2011).
[39] S. Combrié, P. Coman, N.V.Q. Tran, M. Patterson, G. Demand, S. Hughes, R. Gabet, Y. Jaouren, J. Bourderionnet and A. De Rossi, 'Toward a miniature optical true-time delay line', SPIE Newsroom, (2010).
[40] M. H. Khan, H. Shen, Y. Xuan, L. Zhao, S. Xiao, D. E. Leaird, A. M. Wiener, and M. Qi, "Ultrabroad-bandwidth arbitrary radiofrequency waveform generation with a silicon photonic chip-based spectral shaper," Nat. Photonics Vol. 4, pp.117–122 (2010).
[41] Q. Vy Tran, S. Combrié, P. Colman, and A. De Rossi, "Photonic crystal membrane waveguides with low insertion losses," Appl. Phys. Lett., vol. 95, pp. 061105, 2009.
[42] S. Combrie, A. De Rossi, L. Morvan, S. Tonda, S. Cassette, D. Dolfi, and A. Talneau, "Time-delay measurement in singlemode, low-loss photonic crystal waveguides," Electron. Lett., vol. 42, pp. 86-88, 2006
[43] D. B. Hunter and R. A. Minasian, "Tunable microwave fiber-optic bandpass filters," IEEE Photon. Technol. Lett., vol. 11, pp. 874–876, 1999.
[44] D. Van Thourhout, T. Spuesens, S. Kumar, G. Roelkens, R. Kumar, G. Morthier, P. Rojo-Romeo, F. Mandorlo, P. Regreny, O. Raz, C. Kopp and L. Grenouillet, "Nanophotonic devices for optical interconnect," J. Select. Top. Quantum Electron., vol. 16, pp. 1363-1375, 2010.
[45] J. Lloret, G. Morthier, F. Ramos, S. Sales, D. Van Thourhout, T. Spuesens, N. Olivier J.-M. Fedeli and J. Capmany, "Broadband microwave photonic fully tunable filter using a single heterogeneously integrated III-V/SOI-microdisk-based phase shifter", Optics Express, vol. 20, no. 10, pp. 10796-10806, 2012.

Biographies

José Capmany was born in Madrid, Spain, on December 15 1962. He received the Ingeniero de Telecomunicacion degree from the Universidad Politécnica de Madrid (UPM) in 1987 and the Licenciado en Ciencias Físicas in 2009 from UNED. He holds a PhD in Electrical Engineering from UPM and a PhD in Quantum Physics from the Universidad de Vigo.

Since 1991 he is with the Departamento de Comunicaciones, Universidad Politecnica de Valencia (UPV), where he started the activities on optical communications and photonics, founding the Optical Communications Group (www.gco.upv.es). He has been an Associate Professor from 1992 to 1996, and Full Professor in optical communications, systems, and networks since 1996. In parallel, he has been Telecommunications Engineering Faculty Vice-Dean from 1991 to 1996, and Deputy Head of the Communications Department since 1996. Since 2002, he is the Director of the ITEAM Research Institute, Universidad Politécnica de Valencia. His research activities and interests cover a wide range of subjects related to optical communications including optical signal processing, ring resonators, fiber gratings, RF filters, SCM, WDM, and CDMA transmission, wavelength conversion, optical bistability and more recently quantum cryptography and quantum information processing using photonics. He has published over 420 papers in international refereed journals and conferences and has been a member of the Technical Programme Committees of the European Conference on Optical Communications (ECOC), the Optical Fiber Conference (OFC), the Integrated Optics and Optical Communications Conference (IOOC), CLEO Europe, and the Optoelectronics and Communications Conference (OECC). Professor Capmany has also carried out activities related to professional bodies and is the Founder and current Chairman of the LEOS Spanish Chapter, and a Fellow of the Institution of Electrical and Electronic Engineers (IEEE), the Optical Society of America (OSA) and the Institution of Electrical Engineers (IEE). He has acted as a reviewer for over 25 SCI journals in the field of photonics and telecommunications.

Professor Capmany is the recipient of the Extraordinary Engineering Doctorate Prize of the Universidad Politécnica de Madrid and the Extaordinary Physics Laurea Prize from UNED. He is an associate Editor of IEEE Photonics Technology Letters.

Salvador Sales (S'93-M'98-SM'04) is Professor at the Departamento de Comunicaciones, Universidad Politécnica de Valencia, SPAIN. He is also working in the ITEAM Research Institute. He received the degree of Ingeniero de Telecomunicación and the Ph.D. in Telecomunicación from the Universidad Politécnica de Valencia. He is currently the coordinator of the Ph.D. Telecomunicación students of the Universidad Politécnica de Valencia. He has been Faculty Vicedean of the UPVLC in 1998 and Deputy Director of the Departamento de Comunicaciones in 2004-2008. He received the Annual Award of the Spanish Telecommunication Engineering Association to the best PhD. on optical communications. He is co-author of more than 80 journal papers and 150 international conferences. He has been collaborating and leading some national and European research projects since 1997. His main research interests include optoelectronic signal processing for optronic and microwave systems, optical delay lines, fibre Bragg gratings, WDM and SCM ligthwave systems and semiconductor optical amplifiers.

Ivana Gasulla received the M. Sc. degree in Telecommunications Engineering and the Ph.D. degree from the Universidad Politecnica de Valencia (UPV), respectively, in 2005 and 2008. Her PhD thesis was recognized with the IEEE/LEOS Graduate Student Fellowship Award. From 2005 to 2011, she was working at the Optical and Quantum Communications Group of the ITEAM Research Institute. After being awarded a Fulbright Post-Doctoral Fellowship, she is currently carrying out research at Stanford University on spatial multiplexing in multimode optical fibers.

Her research interests are mainly focused on Microwave Photonics, including broadband radio over transmission through multimode fiber links and the application of Slow and Fast Light effects in microwave photonics systems.

José Mora was born in Torrent, Valencia, Spain, on 1976. He received the M. Sc. in Physical Sciences from the Universidad de Valencia (Spain) in 1999. From 1999 to 2004, he worked in the Deparment of Applied Physic from the Universidad de Valencia. He holds a PhD. degree in Physics from the Universidad de Valencia in 2005 and he received the Extraordinary Doctorate Prize of the Universidad de Valencia in 2006. Since 2004, he joined as a researcher at the Optical and Quantum Communications Group in the Institute of Telecommunications and Multimedia Research Institute (ITEAM) from the Universitat Politècnica de València. He has published more than 100 papers and conference contributions covering a wide range of fields related to fiber bragg gratings for sensing applications, optical signal processing, microwave photonics, optical networks and quantum cryptography using photonic technology.

Juan Lloret was born in Altea, Alacant (Spain) in 1984. He received the M. Sc. degree in Telecommunications Engineering from the Universitat Politècnica de València (UPV) in 2008. During the same year, he joined imec (Belgium), where he was involved in the design of integrated all-optical memories. Since November 2008, he has been with the Optical and Quantum Communications Group at the iTEAM Research Institute, where he is currently working toward his Ph.D. degree in the field of microwave photonics. In 2011, he was a guest researcher at imec under the supervision of Prof. Geert Morthier.

His main research interests include Optical Chaos Encryption, Optical Bistability, Silicon Photonics, PICs, III-V-on-Si, Green Photonics, BioPhotonics, Microwave Photonics and Optical Materials.

Juan Sancho was born in Valencia (Spain) in 1984. He received the M. Sc. degree in Telecommunications Engineering from the Universidad Politecnica de Valencia (UPV) in 2008. Since November 2008, he has been with the Optical and Quantum Communications Group at the iTEAM Research Institute, where he is currently working toward his Ph.D. degree in the field of microwave photonics. In 2011, he was a guest researcher at the École Polytechnique Fédérale de Lausanne (Switzerland) under the supervision of Prof. Luc Thévenaz.

His main research interests include Silicon Photonics, PICs, Energy Efficiency Systems, BioPhotonics, Sensors, Microwave Photonics, Communications Systems, Ultrafast Optics and Optical Materials.